THE EFFECT OF TRANSITION METAL DOPING ON THE STRUCTURE AND PROPERTIES OF TECHNOLOGICALLY IMPORTANT POTASSIUM HYDROGEN PHTHALATE (KHP) CRYSTALS

[1]* S. Parthiban, [2] Subbiah Meenakshisundaram
[1]Assistant Professor, [2] Emeritus Professor
[1,2] Department of Chemistry
[1,2] Annamalai University, Annamalainagar 608 002, Tamilnadu, India

ABSTRACT: A systematic analysis of ruthenium concentration effects (0.055, 1.06 and 1.45 mg L^{-1}) on Ru(III)-doped black colored potassium hydrogen phthalate single crystals grown at 30 °C from aqueous growth solution by slow evaporation solution growth technique (SEST) has been made. Considerable influence of doping ruthenium on the structure, optical properties and morphology of potassium hydrogen phthalate (KHP) are observed. Further, the effects are more pronounced with heavy doping. The effect of substitution of ruthenium for potassium in the KHP crystals has been studied by X-ray diffraction (XRD), infrared (IR) absorption, ultra-violet (UV), scanning electron microscope (SEM), energy dispersive spectroscopy (EDS), integrated coupled plasma (ICP) and second harmonic generation (SHG) measurements. Even though, low quantity doping reduces the SHG conversion efficiency considerably, further addition of ruthenium(III) improves the efficiency to a significant extent. The OH^- infrared absorption spectra reveal that there is a change in the position of absorption band and this observation is in tune with the lattice stress and defective structure by doping. Significant peak shifts and changes in intensity patterns observed in the powder XRD of doped specimens clearly reveal the lattice distortion and the incorporation of ruthenium into the crystal matrix is well confirmed by EDS and ICP measurements. SEM reveals the changes in surface morphology with change in ruthenium concentration of the as-grown specimens.

***Keywords* – characterization, doping, growth from solutions, nonlinear optical materials.**

1. INTRODUCTION

Potassium hydrogen phthalate (KHP) is widely known for its application in the long wave X-ray spectrometers [1–3]. Recently, it is used as a substrate for deposition of thin film of organic nonlinear materials [4, 5]. It is a non-centrosymmetric crystal belongs to orthorhombic system with the space group $Pca2_1$, C_{2v}^5 (Z = 4) [6]. Dopants are intentionally incorporated into the crystal structure in order to optimize the physical properties and generally lead to the generation of a charge transfer process [7]. The properties of KHP crystals doped with different elements such as sodium, lithium, rubidium ions [8] and Fe^{3+} and Cr^{3+} [9] are already investigated. Ruthenium (4d element) is chosen as dopant in the present study since it has been established that it improves the sensitivity of $KNbO_3$ for red light [10]. The optical and holographic measurements of ruthenium doped BTO crystals strongly depend on [Ru] [7]. It has been reported that 1% Ru^{4+} doping induces the ferromagnetism and an insulator-metal transition [11, 12]. The ruthenium ion doping on many nonlinear crystals such as $BaTiO_3$ [13], $Bi_{12}TiO_{20}$ [7], $Bi_4Ge_3O_{12}$ [14], $Bi_{12}SiO_{20}$ [15] and $LiNbO_3$ [16] has been reported and it is observed that ruthenium ions can be helpful to improve the photo refractive properties. Ruthenium acts as a promoter for low temperature crystallization of nanostructured tin oxide besides sensitizer [17]. Further, it has been well established that concentration of ruthenium governs the particle size as well as strain in nanocrystalline SnO_2 [18].

In this manuscript, we are reporting for the first time, preliminary experimental results for the effect of doping various ruthenium concentrations on the structure, optical properties and morphology of Ru:KHP crystals. Comparison of results with pure KHP is also made and some useful conclusions have been reached.

2. EXPERIMENTAL

2.1. Crystal growth

Pure and doped KHP crystals with different concentrations of ruthenium [1 mol% (low, *l*), 10 mol% (medium, *m*) and 25 mol% (heavy, *h*)] in aqueous medium are grown by slow evaporation solution growth technique (SEST) at 30 °C. Ruthenium was doped into the aqueous growth medium in the form of dissolved solution of $RuCl_3$ in HCl (0.001 N). The doped crystals are black in color and the color intensifies with doping. Attempts to make still heavier doping (> 25 mol%) of ruthenium on KHP are not successful since the quality of the grown crystals are bad and also, the secondary nucleation could not be controlled. The grown crystals were

harvested from the aqueous growth medium after attaining a reasonable size. Best quality seed crystals are used in the preparation of bulk crystals. After the growth, the crystals were kept in a desiccator. Photographs of pure and various concentrations of Ru(III)-doped KHP crystals are shown in Fig. 1.

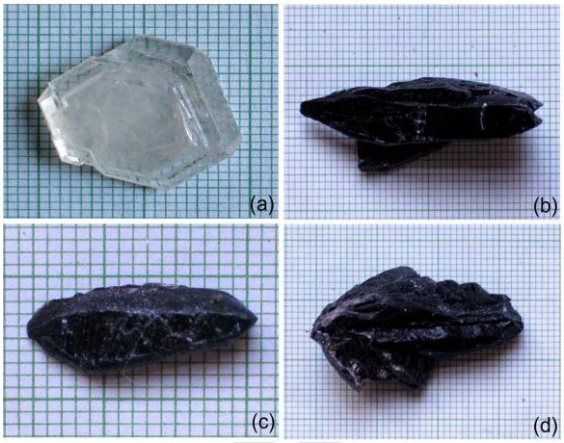

Fig. 1 Photographs of KHP crystals: (a) pure, (b) Ru:KHP (*l*), (c) Ru:KHP (*m*) and (d) Ru:KHP (*h*)

2.2. Characterization

The FT-IR spectra were recorded using AVATAR 330 FT-IR by KBr pellet technique. The single crystal X-ray diffraction studies were performed by using Bruker Axs (Kappa Apex II) X-ray diffractometer. The powder X-ray diffraction was performed by using Philips Xpert Pro Triple-axis X-ray diffractometer. The samples were examined with CuKα radiation in the 2θ range from 10° to 70°. The XRD data is analyzed by Rietveld method with RIETAN–2000. The incorporated ruthenium content in the Ru:KHP specimens were analyzed by ICP–OES 300 spectrometer. Morphologies of the samples and the presence of ruthenium in the specimen were observed by using JEOL JSM 5610 LV scanning electron microscope which has a resolution of 3.0 nm and an acceleration voltage of 0.3 to 30 kV having the maximum magnification of 3,00,000 times. The standard used to study the EDS is cobalt. This instrument can detect elements atomic number from 11 to 92. The Kurtz powder SHG instrument [19] was used for testing SHG.

3. RESULTS AND DISCUSSION

3.1. FT-IR spectra

FT-IR spectra of pure and various concentrations of ruthenium-doped KHP crystals are shown in Fig. 2. A close observation of FT-IR spectra reveal that partial substitution of ruthenium for potassium generally gives rise to small shift of vibrations. FT-IR was used to examine the OH^- absorption spectra of pure and Ru:KHP specimens from 3600–3400 cm^{-1}. The absorption shifts considerably for Ru:KHP specimen with heavy Ru content (Fig. 3). Absorption centered at ~3444 cm^{-1} is typical of the ν_s(O–H) in –COOH stretching vibration. This absorption is shifted to lower wave number (~3376 cm^{-1}) in the heavily Ru(III)-doped specimen. Owing to electrostatic attraction between ruthenium ions and OH^-, stretching of O–H bond takes place and causes a peak shift to lower wave number. The change in position of OH^- absorption band roughly indicates the ruthenium substitution for potassium in the KHP crystal. No appreciable shifts in carbonyl and carboxylate anion stretching vibrations are observed. It appears that replacing Ru by K partially has some effect only in O–H bond. This could be due to the small radius of Ru(III) (82 pm) in comparison with that of potassium ion (152 pm) [20]. Interestingly, Fe-doped $LiNbO_3$ [21] studies reveal that absorption is shifted to shorter wavelengths (higher wave number) due to the displacement of Nb^{5+} by Fe^{2+} in contrast to the present study in which Ru^{3+} replaces K^+. In the present investigations, to preserve the electroneutrality there should be some cation vacancies. Hence, crystal will be more defective which may cause the change in physical properties.

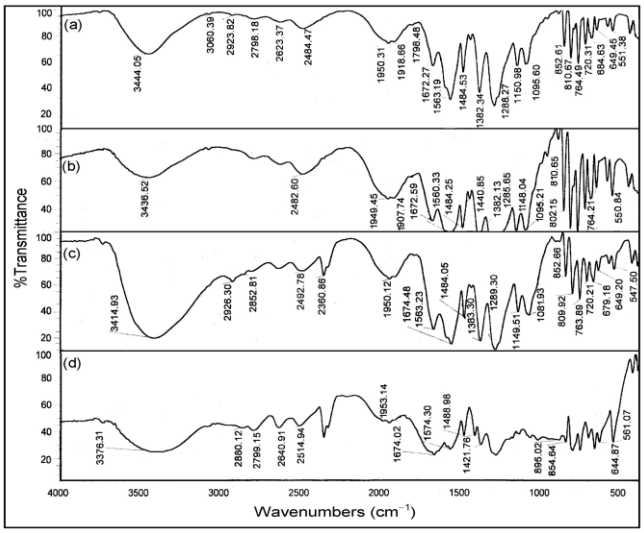

Fig. 2 FT-IR spectra of KHP crystals: (a) pure, (b) Ru:KHP (*l*), (c) Ru:KHP (*m*) and (d) Ru:KHP (*h*)

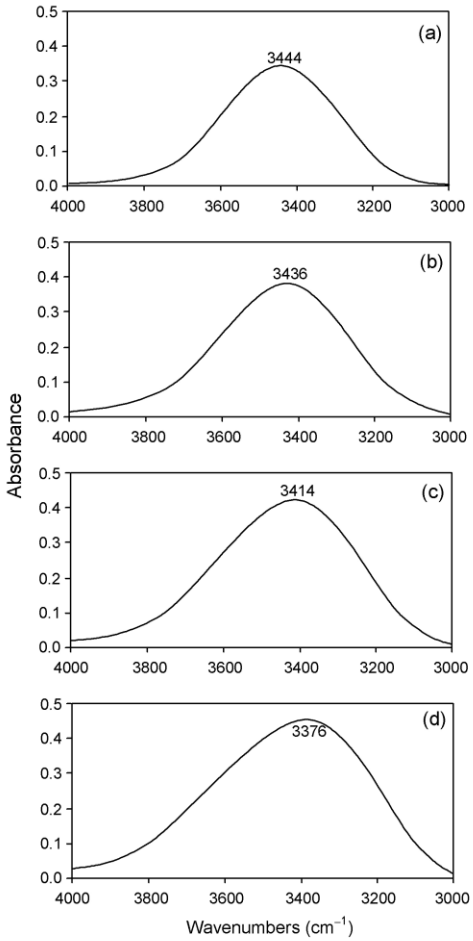

Fig. 3 OH^- IR spectra of KHP crystals: (a) pure, (b) Ru:KHP (*l*), (c) Ru:KHP (*m*) and (d) Ru:KHP (*h*)

3.2. Single crystal and powder XRD analysis

The single crystal X-ray diffraction analysis of pure KHP and Ru:KHP crystals were carried out and this quantitative data (Table 1) shows that there is a small but a gradual increase in lattice constants (*a*, *b* and *c*) and unit cell volume as the [Ru] increases. Near constancy of *a*/*c* values roughly indicate the uniform stress. Since the lattice parameter variations by doping are small, the values are also taken for pure specimen under the experimental conditions and compared with that of available data.

Table 1 Values of lattice constants *a* (Å), *b* (Å), *c* (Å), cell volume $(Å)^3$, *a*/*c* ratio, crystallite size (nm) and effective particle size (nm)

Property	KHP (JCPDS No. 0-031-1855)	Pure KHP	Ru:KHP (*l*)	Ru:KHP (*h*)

a	6.4820	6.48	6.50	6.53
b	9.6120	9.60	9.63	9.68
c	13.3290	13.32	13.35	13.41
v	830.46	830	836	846
a/*c*	0.0078	0.0078	0.0077	0.0077
Crystallite size	–	44	40	66
Effective particle size	–	68.0	25.0	19.35

The powder XRD patterns of the Ru(III)-doped KHP samples are compared with that of the pure one (Fig. 4). General observation is, the relative intensities have been reduced as a result of doping. The preferred orientations are not same for pure and doped specimens. The shift in peak positions and peak broadening as a result of doping are clearly seen in Fig. 5. The interplanar spacing '*d*' shift and broadening in the X-ray lines indicate the presence of uniform and non-uniform strain [18]. Averaged dimension of crystallites (*t*) are calculated using Scherrer equation,

$t = K\lambda / (\beta \cos \theta)$

where *K* is Scherrer constant; λ is the wavelength of X-ray, θ is the peak position measured in radian and β is the integral breadth of reflections (in radian 2θ) located at 2θ. The granularity of the crystal increases from 44 to 66 nm by heavy doping. It appears that the ruthenium doping does not inhibit the growth of the crystals. The ionic radius of the dopant ruthenium (82 pm) is very small compared with that of *K* (152 pm) and hence it is reasonable to believe that ruthenium occupies predominantly substitutional positions, without causing much distortion. Partial substitution of potassium ion by Ru(III) leads to the formation of cation vacancies to maintain the electrical neutrality. Such vacancies cause some broadening in the diffraction peaks and shifts as observed. Analogous type of defect centers with cation vacancy formation is well established in the study of Mn(II)-doped KDP crystals [22] by computer structural modeling and in the investigation of Co(II)-doped tris(thiourea)copper(I) chloride crystals [23]. The observed influences of doping on physical properties could be due to these defective centers to an extent. The effective strain (η) and effective particle size (ε) taking strain into account is estimated using the Hall equation (Fig. 6)

$\beta \cos\theta/\lambda = 1/\varepsilon + \eta \sin\theta/\lambda$

where ε and η are the effective particle size and effective strain. The effective particle size taking strain into account is estimated by plotting $\beta \cos\theta/\lambda$ *versus* $\sin\theta/\lambda$. Negative slope indicates the presence of effective compressive strain in the crystal lattice while a positive slope for Ru:KHP (*l*) and pure KHP is attributed to the presence of tensile strain.

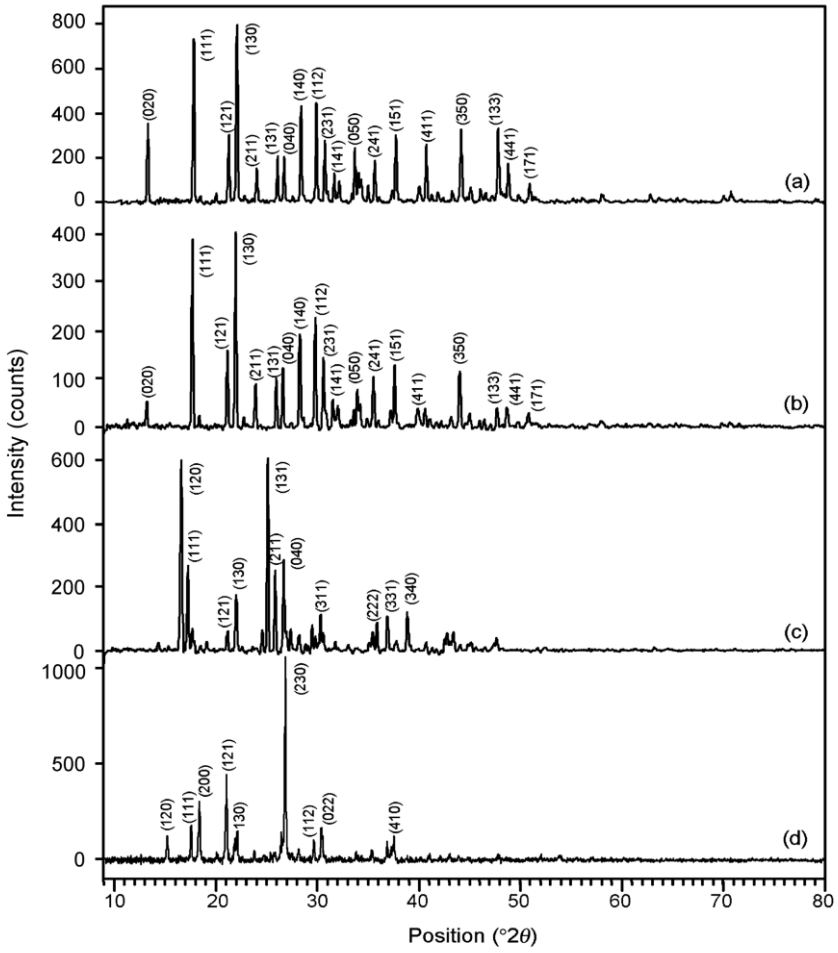

Fig. 4 Powder XRD of KHP crystals: (a) pure, (b) Ru:KHP (*l*), (c) Ru:KHP (*m*) and (d) Ru:KHP (*h*)

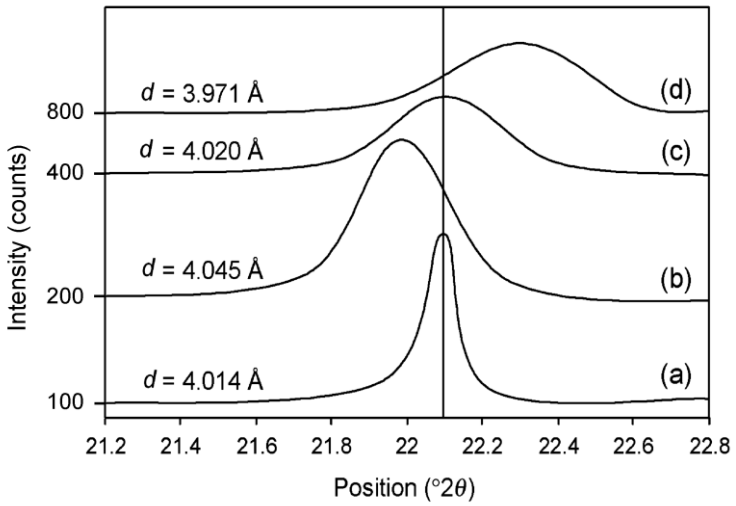

Fig. 5 Peak shift of (130) plane of KHP crystals: (a) pure, (b) Ru:KHP (*l*), (c) Ru:KHP (*m*) and (d) Ru:KHP (*h*)

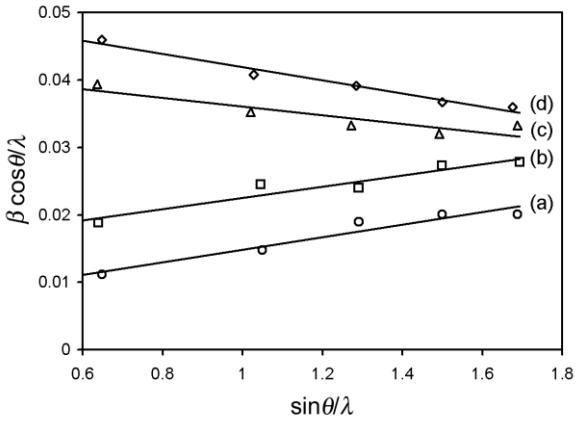

Fig. 6 Plot of $\beta \cos\theta/\lambda$ *versus* $\sin\theta/\lambda$ of KHP crystals: (a) pure, (b) Ru:KHP (*l*), (c) Ru:KHP (*m*) and (d) Ru:KHP (*h*)

3.3. UV-Vis spectra

Absorption in the UV/Vis region is measured from 200 to 1100 nm for pure and doped crystals with various concentrations of Ru (~0.055 to ~1.5 mg L^{-1}) in Ru:KHP (Fig. 7). The UV spectrum reveals that the cut off wavelength is ~310 nm. Doping does not destroy the optical transmission and absorption is minimum in the 300–1100 nm region. A close scan of UV spectra reveal that the absorption edges slightly shift toward longer wavelength region as the [Ru] increases. It could be due to the enhanced defect density of doped specimens. It has been reported that the transmission edge of $Bi_{12}TiO_{20}$ single crystals shifting to the longer wavelength region (IR shift) with increased absorption coefficient is due to the photochromism [7].

The presence of point defects or doping ions in the crystal structure leads to the generation of a charge transfer process responsible for photochromism and photo refractive effect. The photochromism in sillenites is associated with the presence of dopants [7]. Similar photochromic effect is not ruled out in the present study but it has to be verified by annealing and further confirmation is required.

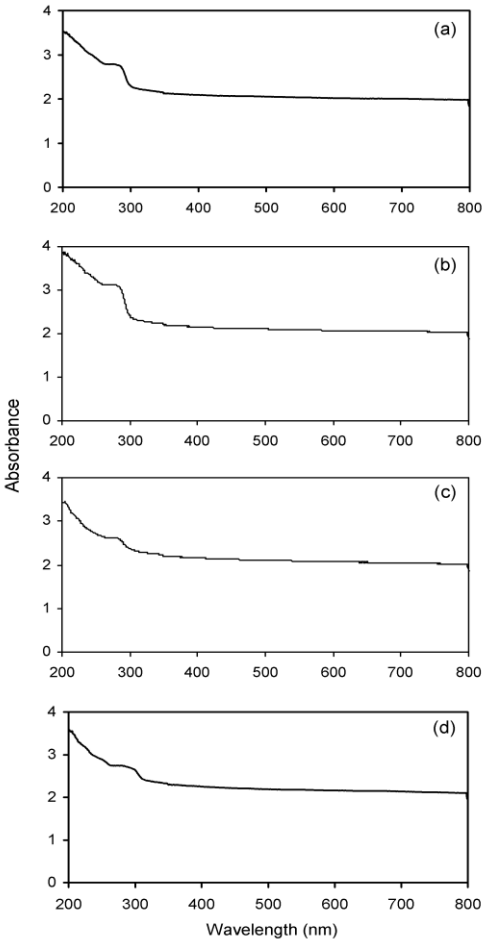

Fig. 7 UV-Vis spectra of KHP crystals: (a) pure, (b) Ru:KHP (*l*), (c) Ru:KHP (*m*) and (d) Ru:KHP (*h*)

3.4. SEM and EDS

The effect of influence of various concentrations of Ru(III) dopant, on the surface morphology of KHP crystal faces reveals structure defect centers as seen in the SEM pictures (Fig. 8). It is clear that the dopant concentration has played a role in changing the morphology of doped specimens. Plate morphology is observed for pure KHP. Doping results in small minute defect centers (low doping), layered structure with deep crack developments (medium doping) and patches with crystal voids (heavy doping). To confirm the incorporation of Ru(III) into the crystalline matrix EDS was performed. The [Ru(III)] in the doped specimen, Ru:KHP increases with increase in the dopant concentration in the aqueous growth medium (Fig. 9). Analysis of surface at different sites indicates that the incorporation is not uniform over the surface.

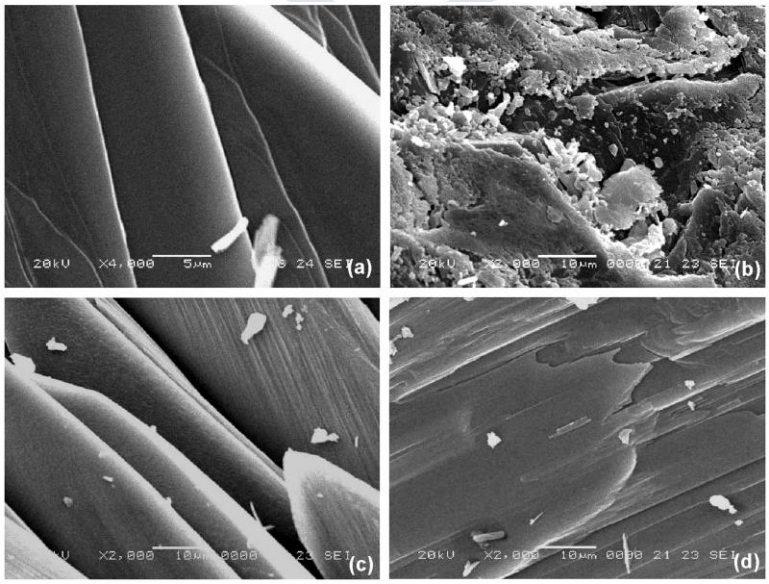

Fig. 8 SEM micrographs of KHP crystals: (a) pure, (b) Ru:KHP (*l*), (c) Ru:KHP (*m*) and (d) Ru:KHP (*h*)

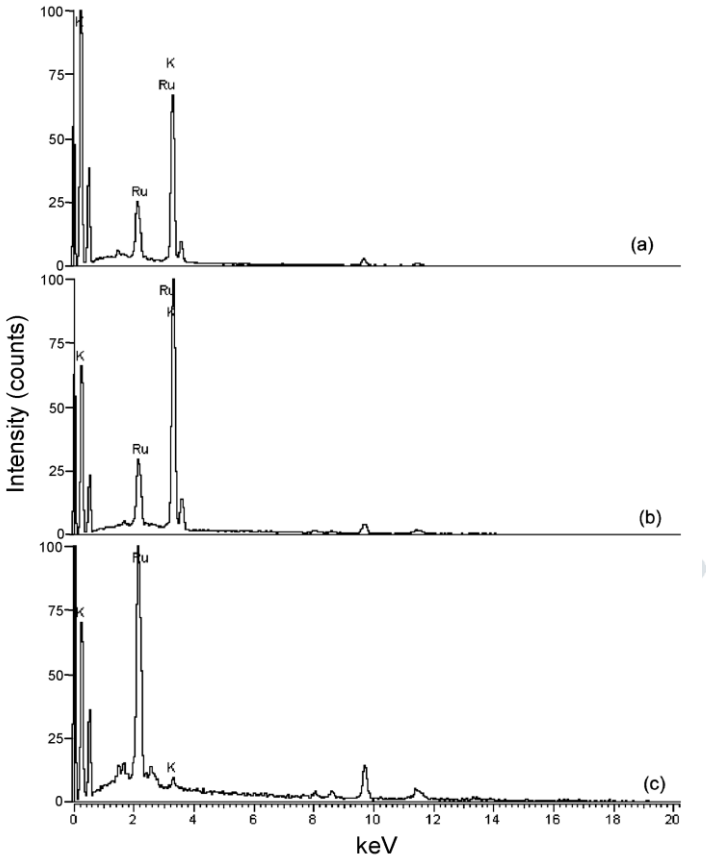

Fig. 9 EDS of KHP crystals: (a) Ru:KHP (*l*), (b) Ru:KHP (*m*) and (c) Ru:KHP (*h*)

3.5. ICP analysis

The amount of dopant in Ru:KHP specimen is estimated using ICP. It is interesting to observe that even though 1, 10 and 25 mol% of Ru(III) were introduced into the aqueous growth medium of KHP, the ICP measurements show that only a small quantity of ruthenium is incorporated into the KHP crystalline matrix (Table 2).

Table 2 Doping concentrations and actual concentrations

Doping concentration of Ru(III) in the aqueous growth medium of KHP	**Actual dopant concentration in the crystalline matrix as determined by ICP (mg L^{-1})**
Ru:KHP (*l*, 1 mol%)	0.055
Ru:KHP (*m*, 10 mol%)	1.06
Ru:KHP (*h*, 25 mol%)	1.45

3.6. SHG efficiency

In order to confirm the influence of doping on the NLO properties, the as grown crystals were subjected to SHG test. The output SHG intensities for pure and doped specimens give relative NLO efficiencies of the measured specimen. It is clearly seen from the Table 3 that doping has a considerable influence on the NLO properties of the KHP crystals. It is interesting to observe that the nonlinearity is not facilitated by doping. Dramatic decrease in SHG efficiency was observed at low [dopant]. However, the conversion efficiency improves considerably with heavy ruthenium content in Ru:KHP crystals. Depressed SHG output in the doped specimens could be due to the deterioration of crystalline perfection that might lead to the disturbance of charge transfer.

Table 3 SHG output

System	**$I_{2\omega}$ (mV)**
Pure KHP	310

Ru:KHP (*l*)	25
Ru:KHP (*h*)	86

4. CONCLUSION

The color, lattice parameters, XRD intensities, peak positions, crystallite size, effective particle size, morphology, SHG conversion efficiency, OH^- IR absorption band and the shift in absorption edge-all these observations depend on the dopant Ru(III) concentration. The effect is more pronounced with heavy doping. Desired properties can be engineered by controlling the ruthenium content in the Ru:KHP crystalline matrix. Results very much suggest that there is a good relationship between the properties of the host material, KHP and dopant induced defects, which depend upon the concentration.

REFERENCES

[1] Jones, J.L., Paschen, K.W. and Nicholson, J.B. 1963. Performance of curved crystals in the range 3 to 12A. Applied Optics, 2: 955–961.

[2] Yoda, O., Miyashita, A., Murakami, K., Aoki, S. and Yamaguchi, N. 1991. Time-resolved X-ray absorption spectroscopy apparatus using laser plasma as an X-ray source. Proceedings of the SPIE - The International Society for Optical Engineering, 1503: 463–466.

[3] Kejalakshmy, N. and Srinivasan, K. 2003. Electro-optic properties of potassium hydrogen phthalate crystal and its application as modulators. Journal of Physics D, 36: 1778–1782.

[4] Nisoli, M., Pruneri, V., Magni, V., De Silvestri, S., Dellepiane, G., Comoretto, D., Cuniberti, C. and Le Moigne, J. 1994. Ultrafast exciton dynamics in highly oriented polydiacetylene films. Applied Physics Letters, 65: 590–592.

[5] Timpanaro, S., Sassella, A., Borghesi, A., Porzio, W., Fontaine, P. and Goldmann, M. 2001. Crystal structure of epitaxial quaterthiophene thin films grown on potassium acid phthalate. Advanced Materials, 13: 127–130.

[6] Mavrin, B.N., Koldaeva, M.V., Zakalumin, R.M. and Turskaya, T.N. 2005. Fourier-Raman spectra of alkali metal and thallium hydrogen phthalate single crystals. Condensed Matter Materials Science. http://arxiv.org/ftp/cond-mat/papers/0504/0504521.pdf

[7] Marinova, V., Hsieh, M.L., Lin, S.H. and Hsu, K.Y. 2002. Effect of ruthenium doping on the optical and photorefractive of $Bi_{12}TiO_{20}$ single crystals. Optics Communications, 203: 377–384.

[8] Hottenhuis, M.H.J. and Lucasius, C.B. 1988. The role of impurities on the process of growing potassium hydrogen phthalate crystals from solution; A quantitative approach. Journal of Crystal Growth, 91: 623–631.

[9] Hottenhuis, M.H.J. and Lucasius, C.B. 1986. The influence of impurities on crystal growth; *In situ* observation of the {010} face of potassium hydrogen phthalate. Journal of Crystal Growth, 78: 379–388.

[10] Buse, K., Hesse, H., van Stevendaal, U., Loheide, S., Sabbert, D. and Kratzig, E. 1994. Photorefractive properties of ruthenium-doped potassium niabate. Applied Physics A, 59: 563–567.

[11] Vijayasarathy, K. and Sreeraj, P. 2002. Effect of ruthenium doping on the properties of $Pr_{0.5}A_{0.5}MnO_3$ (A = Ca, Sr). Solid State Communications, 122: 385–388.

[12] Thanh, P.Q., Cong, B.T., Xuan, C.T.A. and Luong, N.H. 2007. Melting of the charge-ordering state by ruthenium in $Ca_{0.6}Pr_{0.4}Mn_{1-y}Ru_yO_3$ (y = 0, 0.03, 0.05, 0.07) perovskites. Journal of Magnetism and Magnetic Materials, 310: e720–e722.

[13] Lin, C.H., Huang, C.Y. and Chang, J.Y. 2003. Increasing the conductivity of photorefractive $BaTiO_3$ single crystals by doping Ru. Applied Surface Science, 208: 340–344.

[14] Marinova, V., Lin, S.H., Hsu, K.Y., Hsieh, M.L., Gospodinov, M.M. and Sainov, V. 2003. Optical and holographic properties of $Bi_4Ge_3O_{12}$ crystals doped with ruthenium. Journal of Materials Science: Materials in Electronics, 14: 857–858.

[15] Ramaz, F., Rakitina, L., Gospodinov, M. and Briat, B. 2005. Photorefractive and photochromic properties of ruthenium-doped $Bi_{12}SiO_{20}$. Optical Materials, 27: 1547–1559.

[16] Fujimura, R., Shimura, T. and Kuroda, K. 2003. Nonvolatile holographic recording in Ru doped $LiNbO_3$ crystals. In: Delaye, P., Denz, C., Mager, L. and Montemezzani, G. (eds.). Photorefractive Effects, Materials, and Devices. OSA Trends in Optics and Photonics, La Colle sur Loup, France, 87: 660–665.

[17] Ramgir, N.S., Mulla, I.S. and Vijayamohanan, K.P. 2004. Shape selective synthesis of unusual nanobipyramids, cubes and nanowires of RuO_2:SnO_2. Journal of Physical Chemistry B, 108: 14815–14819.

[18] Ramgir, N.S., Hwang, Y.K., Mulla, I.S. and Chang, J.S. 2006. Effect of particle size and strain in nanocrystalline SnO_2 according to doping concentration of ruthenium. Solid State Sciences, 8: 359–362.

[19] Kurtz, S.K. and Perry, T.T. 1968. A powder technique for the evaluation of nonlinear optical materials. Journal of Applied Physics, 39: 3798–3813.

[20] Shannon, R.D. 1976. Revised effective ionic radii and systematic studies of interatomic distances in halides and chalcogenides. Acta Crystallographica A, 32: 751–767.

[21] Bhagavannarayana, G., Ananthamurthy, R.V., Budakodi, G.C., Kumar, B. and Bartwal, K.S. 2005. A study of the effect of annealing of Fe-doped $LiNbO_3$ by HRXRD, XRT and FT-IR. Journal of Applied Crystallography, 38: 768–771.

[22] Rak, M., Eremin, N.N., Eremina, T.A., Kuznetsov, V.A., Okhrimenko, T.M., Furmanova, N.G. and Efremova, E.P. 2005. On the mechanism of impurity influence on growth kinetics and surface morphology of KDP crystals-I: Defect centres formed by bivalent and trivalent impurity ions incorporated in KDP structure-theoretical study. Journal of Crystal Growth, 273: 577–585.

[23] Bhagavannarayana, G., Kushwaha, S.K., Parthiban, S., Ajitha, G. and Meenakshisundaram, S.P. 2008. Influence of inorganic and organic additives on the crystal growth, properties and crystalline perfection on tris(thiourea)copper(I) chloride (TCC) crystals. Journal of Crystal Growth, 310: 2575–2583.